Dispersive Dam-Break Flow of a Photon Fluid

Gang Xu,* Matteo Conforti, Alexandre Kudlinski, and Arnaud Mussot
Univ. Lille, CNRS, UMR 8523—PhLAM—Physique des Lasers Atomes et Molécules, F-59000 Lille, France

Stefano Trillo†
Department of Engineering, University of Ferrara, Via Saragat 1, 44122 Ferrara, Italy

(Received 22 March 2017; published 20 June 2017)

We investigate the temporal photonic analogue of the dam-break phenomenon for shallow water by exploiting a fiber optics setup. We clearly observe the decay of the steplike input (photonic dam) into a pair of oppositely propagating rarefaction wave and dispersive shock wave. Our results show evidence for a critical transition of the dispersive shock into a self-cavitating state. The detailed observation of the cavitating state dynamics allows for a fully quantitative test of the Whitham modulation theory applied to the universal defocusing nonlinear Schrödinger equation.

DOI: 10.1103/PhysRevLett.118.254101

Introduction.—The laser light propagating in nonlinear media often behaves as a photon fluid [1–9], sharing phenomena that characterise fluid flows such as rogue waves [2], instabilities [3], transition to turbulence [4], coherent [5] and incoherent [6] shock waves, superfluid flow around obstacles [7,8], and droplet- or bubblelike behavior [9]. In regimes described by the defocusing nonlinear Schrödinger equation (NLSE), a distinctive trait of the photon fluid evolution is the formation of dispersive shock waves (DSWs, or undular bores) [5,10–14], fast oscillating wave trains that spontaneously emerge from the tendency to develop a gradient catastrophe [15–17]. DSWs are ubiquitous, being observed in other systems ruled by the NLSE such as cold atom condensates [18] and spin waves [19], as well as in other dispersive hydrodynamic settings involving, e.g., electrons [20], water waves [21], and viscous fluid conduits [22]. A major breakthrough in the analytical description of the DSW is the Whitham modulation theory [15–17,23–25], which, however, assumes DSWs to develop from steplike initial conditions (the Riemann problem), whereas experiments to date have been mostly concerned with smooth or periodic initial conditions. Therefore experiments devoted to investigate the dispersive Riemann problem are of paramount importance for advancing the understanding of dispersive hydrodynamic flows, *a fortiori* for the NLSE where the modulation theory predicts critical transitions in the behavior of the shock [18,25].

In this Letter, we exploit a fiber optics setup to investigate experimentally the Riemann problem associated with an initial step, in the temporal domain, in the optical power. In the absence of any frequency chirp across the jump such a problem is isomorphic to the classic 1D dam-break problem of hydrodynamics [26–28]. Indeed, we demonstrate that the light evolves as a fluid mimicking the basic features of the dam break in shallow water, namely, the decay into a shock and a rarefaction-wave (RW) pair, connected by an expanding plateau. The dispersive character of the shock, however, leads to a critical transition, which is predicted in the framework of Whitham theory [18,25]. Above a critical height of the jump, we report evidence for the onset of self-cavitation, i.e., the appearance of a null point in the optical power. The full experimental characterization of the cavitating state allows, for the first time, for a quantitative comparison with modulation theory.

Theory of dispersive dam break.—The dam-break Riemann problem that we investigate is described by the NLSE that rules the evolution of the temporal envelope field $E(T,Z)$ along the fiber distance Z

$$i\frac{\partial E}{\partial Z}-\frac{k''}{2}\frac{\partial^2 E}{\partial T^2}+\gamma|E|^2E=0, \tag{1}$$

subject to a step initial condition in $T=0$, i.e., $E(T,0)=\sqrt{P_L}$ for $T<0$, and $E(T,0)=\sqrt{P_R}$ for $T>0$, where the constant left and right power levels P_L and $P_R\geq P_L$ define the bottom and the top of the optical dam in $T=0$ [see Fig. 1(a)]. Here $T=T_{\rm lab}-k'Z$ is the retarded time in a frame moving with group-velocity $1/k'=dk/d\omega|_{\omega_0}^{-1}$, whereas $k''=d^2k/d\omega^2|_{\omega_0}=176\,\mathrm{ps}^2/\mathrm{km}$ and $\gamma=3\,(\mathrm{Wkm})^{-1}$ are the dispersion and the nonlinear coefficient of our fiber, ω_0 being the carrier frequency. $\gamma k''>0$ corresponds to the defocusing regime of the NLSE. The Madelung transform $E(T,Z)=\sqrt{P_R}\sqrt{\rho(t,z)}\exp\left(-i\int_{-\infty}^{t}u(t',z)dt'\right)$ allows us to formulate the NLSE in hydrodynamical form:

$$\rho_z+(\rho u)_t=0; \tag{2}$$

$$u_z+\left(\frac{u^2}{2}+\rho\right)_t=\frac{1}{4}\left(\frac{\rho_{tt}}{\rho}-\frac{(\rho_t)^2}{2\rho^2}\right)_t, \tag{3}$$

where we set $z=Z/Z_0$, $t=T/T_0$ with $Z_0\equiv(\gamma P_R)^{-1}$, and $T_0\equiv\sqrt{k''/\gamma P_R}$. By neglecting the right-hand side (RHS) containing higher-order derivatives (quantum pressure term

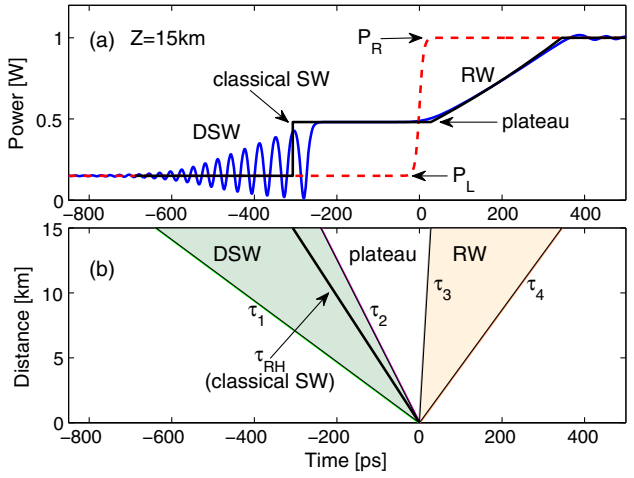

FIG. 1. (a) Snapshots comparing the DSW-RW pair (solid blue curve) obtained from the NLSE with steplike input $E(T,0) = \{P_L + (P_R - P_L)[1 + \tanh(T/T_r)]/2\}^{1/2}$ (dashed red) with the ideal dispersionless solution of the SWEs (solid black). The oscillations over the top of the RW are due to the Gibbs phenomenon [35]. (b) Wedges in (T, Z) plane corresponding to the RW (fable orange), the DSW (green), and the plateau in between. The boundaries correspond to slopes $\sqrt{k''\gamma P_R}\tau_j$, $j = 4$, 3, 2, 1. Here $k'' = 176$ ps^2/km, $\gamma = 3$ (W km)$^{-1}$, $P_R = 1$ W, $P_L = 150$ mW, $T_r = 10$ ps.

[5]), Eqs. (2)–(3) constitute the dispersionless vector conservation law known as the shallow water equations (SWEs) [28]. The role of local water depth and longitudinal velocity are played here by the normalized power $\rho = |E|^2/P_R$ and chirp u, whereas space and time have an interchanged role. The evolution of an initial ($z = 0$) step elevation from ρ_L to $\rho_R > \rho_L$ [29], with $u(t,0)$ identically vanishing, is the classic dam-break Riemann problem. The solution of the SWEs, first given by Stoker [26], can be formulated in terms of the self-similar variable $\tau = t/z$ [30] and involves a classical shock wave and a RW. As shown by the black solid line in Fig. 1(a), the shock and the RW propagate in opposite directions (towards $t < 0$ and $t > 0$, respectively, or the downstream and upstream directions in the hydrodynamic problem), being connected by an expanding plateau characterized by intermediate constant values $\rho_i = (\sqrt{\rho_L} + \sqrt{\rho_R})^2/4$, $u_i = \sqrt{\rho_L} - \sqrt{\rho_R}$. The step values ρ_L and ρ_R also fix the edge velocities of the smooth RW to the values

$$\tau_4 = \sqrt{\rho_R}; \quad \tau_3 = \frac{3\sqrt{\rho_L} - \sqrt{\rho_R}}{2}. \tag{4}$$

Conversely, the jump from ρ_i, u_i to ρ_L, $u_L = 0$ constitutes a classical shock moving with velocity $\tau_{\rm RH} = \rho_i u_i/(\rho_i - \rho_L)$ derived from the well-known Rankine-Hugoniot condition [28]. However, such shock is regularized into an oscillating DSW by the effect of the RHS of Eq. (3) that stems from dispersion. A snapshot of the breaking scenario obtained from the full NLSE is compared with the dispersionless limit (SWEs) in Fig. 1(a). The DSW is delimited by two edge velocities $\tau_{1,2}$ ($\tau_1 < \tau_{\rm RH} < \tau_2$), where the oscillations vanish (linear edge) or become deepest (soliton edge [31]), respectively [15,18,25]. According to Whitham modulation theory such velocities read as [25,32]

$$\tau_2 = -\frac{\sqrt{\rho_L} + \sqrt{\rho_R}}{2}; \quad \tau_1 = \frac{\rho_L - 2\rho_R}{\sqrt{\rho_R}}, \tag{5}$$

whereas, in the same framework, owing to the RW smoothness, one recovers Eqs. (4) for the RW edges. The velocities $\tau_{1,2}$ in Eqs. (5) and $\tau_{3,4}$ in Eqs. (4) define the wedges where the DSW and RW expand, as shown (in dimensional units, i.e., including the multiplicative factor $T_0/Z_0 = \sqrt{k''\gamma P_R}$ for our fiber) in Fig. 1(b). Importantly, the modulation theory entails a crossover between two different regimes separated by a critical condition. In the first regime, the DSW envelopes are monotonic and the DSW power never vanishes, as shown in Fig. 1(a). However, below a critical value of the key parameter, namely, the ratio between the quiescent (downstream and upstream) states, that we henceforth denote as $r = \rho_L/\rho_R = P_L/P_R$, the DSW exhibits a self-cavitating point (i.e., zero power, corresponding to a vacuum point in gas dynamics), which we found at [32]

$$\tau_0 = \sqrt{\rho_L} - \sqrt{\rho_R} + 2\sqrt{\rho_L}\left[1 - \frac{\sqrt{\rho_R} - \sqrt{\rho_L}}{\sqrt{\rho_R} - 3\sqrt{\rho_L}}\frac{E(m)}{K(m)}\right]^{-1}, \tag{6}$$

where E and K are elliptic integrals of the first and second kind, respectively, of modulus $m = 4\rho_L/(\sqrt{\rho_L} - \sqrt{\rho_R})^2$. The threshold for cavitation can be obtained by imposing $m = 1$ (cavitation on soliton edge of the DSW), or, equivalently, $\tau_2 = u_i$, from which we obtain

$$r_{\rm th} \equiv \left(\frac{\rho_L}{\rho_R}\right)_{\rm th} \equiv \left(\frac{P_L}{P_R}\right)_{\rm th} = \frac{1}{9} \simeq 0.11. \tag{7}$$

For P_L/P_R below such threshold, a vacuum point always exists, which tends towards the linear edge of the DSW in the limit $P_L \to 0$. In this limit, however, both the oscillation amplitude and the plateau extension tends to vanish [25], and one recovers the limiting hydrodynamic case known as "dry-bed" dam break, characterized by a single RW extending to zero and no shock [27,33,34].

Experiment.—We performed a series of experiments to provide evidence for the decay of a photonic dam (i.e., a temporal step in optical power) into the DSW-RW pair and for the critical transition to self-cavitation. In our experimental setup (see also Ref. [32]), we make use of a continuous laser diode source emitting at $\lambda = 1560$ nm, which is intensity modulated by an electro-optic modulator driven by an arbitrary waveform generator, with typical rise time $T_r \sim$ 25 ps (raised tanh shape, rising from 10% to 90% in ~50 ps) and 78 MHz repetition rate. The signal is preamplified in a semiconductor optical amplifier, and then it passes through a spectral filter to remove amplified spontaneous emission in

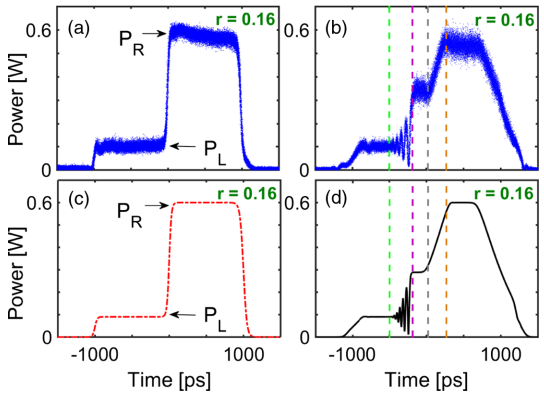

FIG. 2. Temporal traces of the whole waveform: (a),(b) experiment; (c),(d) numerics. The left column (a),(c) shows the input; The right column (b),(d) is the output power profile after propagation along the 15 km long fiber. The vertical dashed lines give the predicted delays of the edges of the RW [gray and orange lines, from Eqs. (4)] and the DSW [magenta and green lines, from Eqs. (5)], respectively.

excess, and is finally amplified by means of an Erbium-doped fiber amplifier. This signal is launched in a dispersion compensating fiber (i.e., a fiber with large positive dispersion), with parameters as in the caption of Fig. 1, and analyzed in the time domain with an optical sampling oscilloscope with 1.6 ps resolution. A typical shape of the steplike signal that we obtained is shown in Fig. 2(a). Two elevating steps in power from zero to P_L and from P_L to P_R, can be adjusted independently, and are followed by a descending step (trailing edge) back to zero. The advantage of using this specific signal shape is that, in the same experimental run, we can compare (i) the DSW-RW dynamics developing around the jump from P_L to P_R, with (ii) the dry-bed dynamics developing over the descending step. Importantly, the duration of each of the constant power states P_L, P_R was adjusted to be long, up to $\sim$1 ns, so that the DSW-RW pair can develop without feeling the interaction with the first step and the trailing edge of the waveform. Clearly, as can be seen in Fig. 2(a), the main step (P_L to P_R) is not instantaneous. However, the short rising time allows us to clearly observe the dam-break phenomenon, as we will see below. Another challenging issue faced in the experiment is the loss compensation. Indeed, the DSW-RW dynamics is very sensitive to losses and even weak losses of optical fibers (0.5 dB/km) are strongly detrimental. For instance, the plateau that connects the RW and the DSW would be completely distorted, not allowing for a quantitative comparison with theory (see Figs. S2 and S3 in Ref. [32]). Inspired from transparent telecom networks, we counterbalanced linear losses by means of Raman amplification [36,37]. To this end, a counterpropagating beam was injected in the fiber at $\lambda = 1482$ nm. In this way, we achieve significant (close to peak) Raman gain with weak relative noise intensity transfer [36,37].

Figure 2(b) shows the output temporal trace obtained for the input steplike signal with $P_R = 0.6$ W, $P_L \simeq 100$ mW ($r \simeq 0.16$). As can be seen, the input optical dam at $T = 0$ breaks into a DSW-RW pair. The DSW is characterized by fast oscillations with $\sim$40 ps average period [the period scales proportionally to $\sqrt{k''/(\gamma P_i)}$]. The RW smoothly connects the plateau with power $P_i \simeq 0.3$ W (in agreement with the theoretical prediction $P_i = P_R\rho_i = 0.297$ W) to the peak level P_R. Conversely, over the trailing edge, no shock occurs and a smooth RW dropping to zero is observed, consistently with the case of dry-bed dam break. Overall, the data show an excellent agreement with the numerical simulations reported in Fig. 2(d) based on the NLSE (1). We emphasize that the occurrence of the DSW-RW pair is related to the nonzero background and not to the character (ascending vs descending) of the step. Indeed the DSW-RW pair is observed on the trailing edge for a mirror-symmetric input.

We have then proceeded to investigate in detail the breaking dynamics of the steplike input into the DSW-RW pair for different heights of the optical dam. The results shown in Fig. 3, are obtained for a fixed peak power $P_R = 0.8$ W (slightly larger than that of Fig. 2), and a variable background P_L, i.e., a variable ratio r. For a quantitative comparison with Whitham modulation theory we also report, as vertical dashed lines superimposed on the measured data, the delays $T_j = \sqrt{k''\gamma P_R}\tau_j L$, $j = 1, 2, 3, 4$ corresponding to the edges of the RWs in Eq. (4) and the DSW in Eq. (5), respectively. We remark that (i) the experimental traces (left column) show a very good agreement with both simulations based on the NLSE (right column), and the predicted delays T_j from modulation theory, (ii) the duration of the plateau connecting the DSW

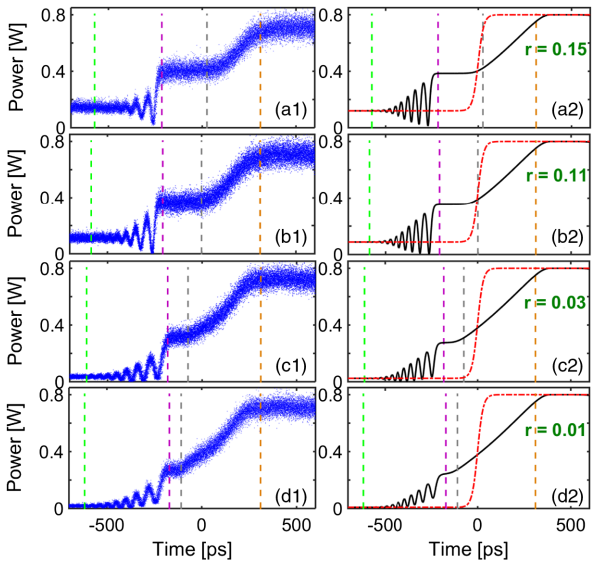

FIG. 3. Temporal traces at the fiber output for constant peak power of the photonic dam $P_R = 0.8W$ and different background fractions r: (a1,a2) 0.15; (b1,b2) 0.11; (c1,c2) 0.03; (d1,d2) 0.01. Left column: experimental results. Right column: numerical simulation based on the NLSE.

and the elevating RW significantly shrinks as the ratio r decreases (from top to bottom in Fig. 3), again in quantitative agreement with modulation theory which predicts that $|\tau_2 - \tau_3|$ reduces when r decreases, and (iii) for relatively large ratios r the DSW never touches zero and the edge τ_2 of the DSW (where $m = 1$) is constituted by a gray soliton [18], as shown in Figs. 3(a1)–3(a2). However, by decreasing r, we observe the onset of cavitation when the soliton at the trailing edge of the DSW becomes black [see Figs. 3(b1), 3(b2), $r = 0.11$]. The observed threshold value $r = 0.11$ is in excellent agreement with the theoretical prediction [Eq. (7)]. While the black soliton possess a zero velocity (with respect to its background), the DSW edge maintains a finite velocity due to the chirped background (velocity u_i). Also associated with such black soliton we expect a phase jump of π [see Fig. S5(b) for more details] which, however, cannot be measured with our setup. At even lower ratios r, the vacuum point shifts towards the left and the DSW envelope becomes nonmonotonic.

While the results in Fig. 3 already show the crossover to the cavitating state, a detailed quantitative study of this regime requires to operate with a DSW possessing larger extension and shorter average period. To this end, we operate at the maximum available power in our setup, $P_R = 1$ W. This allows us to observe a DSW exhibiting several oscillations with an average period of ~30 ps, spanning a range that exceeds 400 ps, as shown in the inset of Fig. 4(e), for $P_L = 50$ mW or $r = 0.05$. Importantly, in this regime the delay of the cavitating state (zero power) can be accurately identified within the DSW. Figures 4(a)–4(d) display a zoom over the bottom part of the DSW in order to show how the cavitating state moves when the ratio r is varied across the threshold. As shown in Figs. 4(a1)–4(a2), when $r = 0.15$, the DSW still exhibits monotonic envelopes featuring a gray soliton edge with nonvanishing dip. However, Figs. 4(b1)–4(b2) show very clearly the onset of cavitation (black soliton edge) at the threshold $r = 0.11$, in agreement with Eq. (7). Decreasing further r (i.e., for higher dam heights) leads the cavitating state to acquire increasingly negative delays, shifting progressively towards the linear edge of the DSW, as clear from Figs. 4(c1)–4(c2) for $r = 0.07$ and Figs. 4(d1)–4(d2) for $r = 0.03$. For all cases the numerical simulations are still in good agreement with the measured profiles. We summarize in Fig. 4(e) the delays of the vacuum state extracted from the measured temporal traces for different ratios r (see also Ref. [32]) in the range $0.01 \leq r \leq r_{\text{th}}$ (below $r \sim 0.01$, the residual noise makes impossible to resolve the delay of the vacuum which is quite close to the linear edge). The data are contrasted with the theoretical prediction from Eq. (6), showing a satisfactory agreement in the whole range. We ascribe the discrepancies to the finite rise-time of the step and to the asymptotic character of Whitham theory, which is expected to become more accurate as the propagation length increases and/or the dispersion decreases [16].

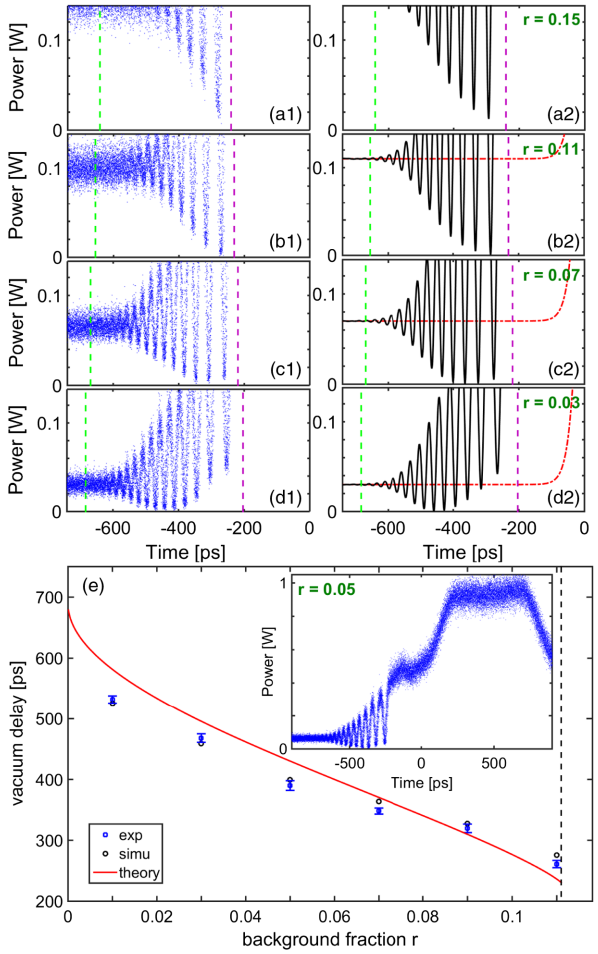

FIG. 4. (a)–(d) As in Fig. 3, showing a zoom around the spontaneously cavitating state (vacuum point) of the DSW, for $P_R = 1$ W and different fractions $r = P_L/P_R$: (a1),(a2) 0.15; (b1),(b2) 0.11; (c1),(c2) 0.07; (d1),(d2) 0.03. (e) Measured delay of the cavitating state vs r, compared with prediction from Eq. (6) and numerical simulations of the NLSE. The dashed vertical line stands for the threshold in Eq. (7). Inset: overall RW-DSW dynamics of the case $r = 0.05$.

In summary, we have reported the fluid behavior of light in a dispersive dam-break experiment, revealing a transition to cavitation in close quantitative agreement with the predictions of modulation theory. Such behavior is expected to be universal for systems ruled by the NLSE, while qualitatively differing from other dispersive breaking scenarios observed in fluids [38]. Our platform could be further used to explore other critical behaviors in the general dispersive Riemann problem [25,39], including the focusing case [40], where a different DSW composed by bright solitons can emerge and can also lead to the generation of rogue waves.

The present research was supported by IRCICA (USR 3380 CNRS), by the Agence Nationale de la Recherche in the framework of the Labex CEMPI (ANR-11-LABX-0007-01), Equipex FLUX (ANR-11-EQPX-0017), by the

projects No. AWE (ANR-14-ACHN-0014), TOPWAVE (ANR-13-JS04-0004), and the Ministry of Higher Education and Research, Hauts de France council and European Regional Development Fund (ERDF) through the Contrat de Projets Etat-Region (CPER Photonics for Society P4S). S. T. acknowledges also the grant PRIN 2012BFNWZ2. The authors are grateful to L. Bigot, E. Andresen and IRCICA-TEKTRONIX European Optical and Wireless Innovation Laboratory for technical support about the electronic devices.

*gang.xu@ircica.univ-lille1.fr
†stefano.trillo@unife.it

[1] M. Brambilla, L. A. Lugiato, V. Penna, F. Prati, C. Tamm, and C. O. Weiss, Phys. Rev. A **43**, 5114 (1991).
[2] M. Onorato, S. Residori, U. Bortolozzo, A. Montina, and F. T. Arecchi, Phys. Rep. **528**, 47 (2013); N. Akhmediev *et al.*, J. Opt. **18**, 063001 (2016).
[3] S. Jia, M. Haataja, and J. W. Fleischer, New J. Phys. **14**, 075009 (2012).
[4] E. G. Turitsyna, S. V. Smirnov, S. Sugavanam, N. Tarasov, X. Shu, S. A. Babin, E. V. Podivilov, D. V. Churkin, G. Falkovich, and S. K. Turitsyn, Nat. Photonics **7**, 783 (2013).
[5] W. Wan, S. Jia, and J. W. Fleischer, Nat. Phys. **3**, 46 (2007).
[6] J. Garnier, G. Xu, S. Trillo, and A. Picozzi, Phys. Rev. Lett. **111**, 113902 (2013).
[7] I. Carusotto and C. Ciuti, Rev. Mod. Phys. **85**, 299 (2013); I. Carusotto, Proc. R. Soc. A **470**, 20140320 (2014).
[8] D. Vocke, K. Wilson, F. Marino, I. Carusotto, E. M. Wright, T. Roger, B. P. Anderson, P. Öhberg, and D. Faccio, Phys. Rev. A **94**, 013849 (2016).
[9] D. Novoa, H. Michinel, and D. Tommasini, Phys. Rev. Lett. **103**, 023903 (2009); A. Paredes, D. Feijoo, and H. Michinel, Phys. Rev. Lett. **112**, 173901 (2014).
[10] C. Conti, A. Fratalocchi, M. Peccianti, G. Ruocco, and S. Trillo, Phys. Rev. Lett. **102**, 083902 (2009).
[11] J. Fatome, C. Finot, G. Millot, A. Armaroli, and S. Trillo, Phys. Rev. X **4**, 021022 (2014).
[12] J. Wang, J. Li, D. Lu, Q. Guo, and W. Hu, Phys. Rev. A **91**, 063819 (2015).
[13] G. Xu, A. Mussot, A. Kudlinski, S. Trillo, F. Copie, and M. Conforti, Opt. Lett. **41**, 2656 (2016).
[14] G. Millot, S. Pitois, M. Yan, T. Hovhannisyan, A. Bendahmane, T. W. Hänsch, and N. Picqué, Nat. Photonics **10**, 27 (2016).
[15] G. A. El and M. A. Hoefer, Physica (Amsterdam) **333D**, 11 (2016).
[16] T. Grava, in *Rogue and Shock Waves in Nonlinear Dispersive Media*, edited by M. Onorato, S. Residori, and F. Baronio, Lecture Notes in Physics (Springer, Berlin, 2016).
[17] A. M. Kamchatnov, *Nonlinear Periodic Waves and Their Modulations—An Introductory Course* (World Scientific, Singapore, 2000).
[18] M. A. Hoefer, M. J. Ablowitz, I. Coddington, E. A. Cornell, P. Engels, and V. Schweikhard, Phys. Rev. A **74**, 023623 (2006).
[19] P. A. P. Janantha, M. A. Hoefer, and M. Wu, arXiv:1610.08846.
[20] Y. C. Mo, R. A. Kishek, D. Feldman, I. Haber, B. Beaudoin, P. G. O'Shea, and J. C. T. Thangaraj, Phys. Rev. Lett. **110**, 084802 (2013).
[21] S. Trillo, G. Deng, G. Biondini, M. Klein, G. F. Clauss, A. Chabchoub, and M. Onorato, Phys. Rev. Lett. **117**, 144102 (2016).
[22] M. D. Maiden, N. K. Lowman, D. V. Anderson, M. E. Schubert, and M. A. Hoefer, Phys. Rev. Lett. **116**, 174501 (2016).
[23] M. V. Pavlov, Theor. Math. Phys. **71**, 584 (1987).
[24] A. V. Gurevich and A. V. Krylov, JETP **65**, 944 (1987).
[25] G. El, V. Geogjaev, A. Gurevich, and A. Krylov, Physica (Amsterdam) **87D**, 186 (1995).
[26] J. J. Stoker, *Water Waves* (Interscience, New York, 1957).
[27] G. B. Whitham, *Linear and Nonlinear Waves* (Wiley, New York, 1974).
[28] R. J. Leveque, *Finite-Volume Methods for Hyperbolic Problems* (Cambridge University Press, Cambridge, England, 2004).
[29] Clearly choosing P_R as the reference power amounts to fix $\rho_R = 1$. However, in order to write more general formulas we leave both ρ_R and ρ_L as free boundary values.
[30] $\tau = t/z$ is referred to as a velocity, as commonly used in shock wave theory, though, dimensionally, this is an inverse velocity.
[31] The modulation theory describes the DSW as a modulated cnoidal wave, which locally reduces to a dark soliton over the deepest dark edge. Naively, the DSW can be seen as a train of dark solitons, but not of bright solitons that do not exist in the defocusing regime.
[32] See Supplemental Material at http://link.aps.org/supplemental/10.1103/PhysRevLett.118.254101 for the derivation of Eqs. (4)–(6), for more details on the experiment along with a sketch of the setup, and for additional experimental results.
[33] J. D. Martin and W. J. Moyce, Phil. Trans. R. Soc. A **244**, 312 (1952).
[34] Y. Kodama and S. Wabnitz, Opt. Lett. **20**, 2291 (1995).
[35] G. Biondini and T. Trogdon, arXiv:1411.6142.
[36] C. Headley and G. P. Agrawal, *Raman Amplification in Fiber Optical Communication Systems* (Academic Press, Amsterdam, 2005).
[37] L. F. Mollenauer, R. H. Stolen, and M. N. Islam, Opt. Lett. **10**, 229 (1985).
[38] A. Treske, J. Hydraul. Res. **32**, 355 (1994); S. Soares-Frazao and Y. Zech, J. Hydraul. Res. **40**, 33 (2002); D.-H. Kim and P. J. Lynett, J. Hydraul. Eng. **137**, 754 (2011).
[39] G. Biondini and Y. Kodama, J. Nonlinear Sci. **16**, 435 (2006).
[40] G. A. El, E. G. Khamis, and A. Tovbis, Nonlinearity **29**, 2798 (2016).